Eleventh International Conference on CFD in the Minerals and Process Industries
CSIRO, Melbourne, Australia
7-9 December 2015

BUBBLE-EMULSION HEAT TRANSFER COEFFICIENT IN GAS-SOLID FLUIDIZED BED USING TWO FLUID MODEL

Mohammad BANAEI[1,2], Martin VAN SINT ANNALAND[1,2], J.A.M. KUIPERS[1,2] and Niels G. DEEN[1,2*]
[1] Multiphase Reactors Group, Department of Chemical Engineering and Chemistry, Eindhoven University of Technology, P.O. Box 513, 5600 MB Eindhoven, the Netherlands

[2] Dutch Polymer Institute (DPI), P.O. Box 902, 5600 AX Eindhoven, The Netherlands
*Corresponding author, E-mail address: N.G.Deen@tue.nl

ABSTRACT

After implementation and verification of energy equations into an existing two fluid model (TFM) code, the bubble-emulsion heat transfer coefficients were calculated for various cases. The simulation results were compared with other theoretical models. At the end, a new correlation based on TFM results for gas fluidized beds with coarse particles is proposed. This equation can be used as an input for large-scale phenomenological models.

NOMENCLATURE

A	Area (m^2)
C_p	Heat capacity (J/kg.K)
d, *D*	Diameter (m)
e	Restitution coefficient
G	Dimensionless gas temperature
g	Gravitational acceleration (m/s^2)
H	Volumetric heat transfer coefficient ($W/m^3.K$)
h	Heat transfer coefficient ($W/m^2.K$)
I_0	Modified Bessel function of the first kind and zero order
KL	Kunii and Levenspiel
k	Heat conductivity (W/m.K)
MW	Molecular weight (kg/kmol)
Nu	Dimensionless Nusselt number
P	Dimensionless solid temperature
Pr	Dimensionless Prandtl number
q	Pseudo-Fourier fluctuating kinetic energy flux (kg/s^3)
Re	Dimensionless Reynolds number
S	Surface (m^2)
T	Temperature (K)
t'	Dimensionless time
TFM	Two fluid model
u	Velocity (m/s)
V	Volume (m^3)
α	Interfacial heat transfer coefficient ($W/m^3.s$)
β	Interphase momentum transfer coefficient ($kg/m^3.s$)
γ	Dissipation of granular energy due to inelastic particle-particle collision ($kg/m.s^3$)
ε	Volume fraction
θ	Granular temperature (m^2/s^2)
μ	Viscosity (Pa.s)
υ	Mass flow rate (m^3/s)
ρ	Density (kg/m^3)
τ	Stress tensor (Pa/m)

SUBSCRIPTS and SUPERSCRIPTS

BE	Bubble-Emulsion
b	Bubble
bc	Bubble-Cloud
bg	Background
e	Emulsion
eff.	Effective
g	Gas
gs	Gas-Solid
init.	Initial
inj.	Injection
mf	Minimum fluidization condition
p	Particle
r	Radial direction
s	Solid
z	Axial direction
θ	Azimuthal direction

INTRODUCTION

Gas-solid fluidized beds are widely applied in the chemical industries. Although much work has been done for predicting and understanding the behaviour of these contactors, many aspects of these contactors are not fully understood yet. Various approaches can be used for getting more insight in the dynamics of gas fluidized beds. Among all these approaches, computational fluid dynamics has become an extremely powerful tool during the last few decades. In this work, the computational two fluid model (TFM) based on the kinetic theory of granular flow (KTGF) was used. TFM is an Eulerian-Eulerian approach that considers the particulate phase as a continuous phase like the gas phase (Kuipers et al., 1993; Nieuwland et al., 1996). Interested readers can refer to the work by Gidaspow (2012) for further details and derivation of the TFM based on the KTGF governing equations.

As heat transfer plays an important role in many gas-fluidized bed applications like combustors, and polymerization reactors (Geng and Che, 2011; Kaneko et al., 1999), we present a method to calculate bubble-emulsion heat transfer coefficients with the aid of the TFM. Simulation results obtained with the TFM were compared with other models and a modified correlation for bubble emulsion heat transfer coefficient was proposed. These results are highly valuable as an input for large-scale phenomenological models.

THEORY

The two-phase flow is governed by the following equations:

$$\frac{\partial}{\partial t}(\varepsilon_g.\rho_g) + \nabla.(\varepsilon_g.\rho_g \vec{u}_g) = 0 \qquad (1)$$

$$\frac{\partial}{\partial t}(\varepsilon_s.\rho_s)+\nabla.(\varepsilon_s.\rho_s\vec{u}_s)=0 \quad (2)$$

$$\frac{\partial}{\partial t}(\varepsilon_g.\rho_g\vec{u}_g)+\nabla.(\varepsilon_g.\rho_g\vec{u}_g\vec{u}_g)= \quad (3)$$
$$-\varepsilon_g\nabla P_g-\nabla.(\varepsilon_g.\bar{\bar{\tau}}_g)-\beta(\vec{u}_g-\vec{u}_s)+\varepsilon_g.\rho_g.\vec{g}$$

$$\frac{\partial}{\partial t}(\varepsilon_s.\rho_s\vec{u}_s)+\nabla.(\varepsilon_s.\rho_s\vec{u}_s\vec{u}_s)= \quad (4)$$
$$-\varepsilon_s\nabla P_g-\nabla P_s-\nabla.(\varepsilon_s.\bar{\bar{\tau}}_s)+\beta(\vec{u}_g-\vec{u}_s)+\varepsilon_s.\rho_s.\vec{g}$$

$$\frac{3}{2}[\frac{\partial}{\partial t}(\varepsilon_s.\rho_s.\theta)+\nabla.(\varepsilon_s.\rho_s.\theta\vec{u}_s)]= \quad (5)$$
$$-(p_s\bar{\bar{I}}+\varepsilon_s\bar{\bar{\tau}}_s):\nabla\vec{u}_s-\nabla.(\varepsilon_s q_s)-3\beta\theta-\gamma$$

$$C_{p,g}\frac{\partial(\varepsilon_g\rho_g T_g)}{\partial t}+C_{p,g}\nabla.(\varepsilon_g\rho_g\vec{u}_g T_g)= \quad (6)$$
$$\nabla.(\varepsilon_g k_g^{eff}\nabla T_g)-\alpha_{gs}(T_g-T_s)$$

$$C_{p,s}\frac{\partial(\varepsilon_s\rho_s T_s)}{\partial t}+C_{p,s}\nabla.(\varepsilon_s\rho_s\vec{u}_s T_s)= \quad (7)$$
$$\nabla.(\varepsilon_s k_s^{eff}\nabla T_s)+\alpha_{gs}(T_g-T_s)$$

Equations (1) and (2) presents the continuity equations for the gas and solid phases, equations (3) and (4) are the momentum balance equations for the gas and solid phases and equation (5) is the balance over granular temperature. The model with these five set of equations was implemented and verified by Verma et al. (2013). Equations (6) and (7) are the heat transfer (energy balance) equations for the gas and solid phases respectively. These two set of equations was implemented and verified in an existing in-house code. Implementation of equations (6) and (7) enable us to find the temperature distribution in the bed for non-isothermal systems. In these equations, the convection terms were discretized with Superbee total variation diminishing (TVD) scheme (Roe, 1986). Common closure relations were used to calculate the frictional viscosity (Srivastava and Sundaresan, 2003), effective thermal conductivity (Biyikli et al., 1988; Zehner and Schlunder, 1970), the interfacial drag (van der Hoef et al., 2005) and interfacial heat transfer coefficient (Gunn, 1978).

To verify the correct implementation of the thermal energy equation in the model, various test cases were performed, each testing different terms in the equation. For the sake of brevity, only the verification of fixed bed test case is presented here. In this test case, a simulation for heat transfer in a 1-D fixed bed was performed. The simulation conditions are listed at Table 1. A schematic representation of this test case is shown in Figure 1. In this test case, the temperature of both the solid and the gas phases are set to $T_{init.}$ at t = 0, at which time hot gas with the temperature T_{inlet} was introduced to the bed. The only heat transport mechanism present in this test is convection and the gas moves through the bed in plug flow. However, it should be mentioned that conduction also occurs in reality but it is ignored in this test. The conduction terms are verified separately. The verification of conduction terms is not presented in this work for brevity. As the density of both phases are constant in this test, the governing equations are as follows,

$$\rho_g C_{p,g}\frac{\partial(\varepsilon_g T_g)}{\partial t}+\rho_g C_{p,g}\frac{\partial}{\partial z}\left(\varepsilon_g u_z T_g\right)=-\alpha_{gs}(T_g-T_s) \quad (8)$$

$$\rho_s C_{p,s}\frac{\partial(\varepsilon_s T_s)}{\partial t}=\alpha_{gs}(T_g-T_s) \quad (9)$$

A comparison of the simulation results and the analytical solution is presented in Figure 2. The analytical solution for this test is presented at Table 2.

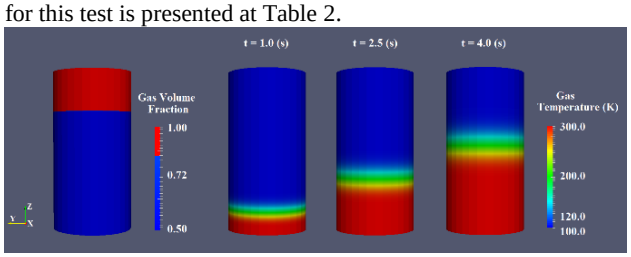

Figure 1: Schematic representation of fixed bed test case.

Table 1: Simulation conditions for fixed bed test case.

Variable	Value	Unit
n_r	3	-
n_θ	8	-
n_z	160	-
$C_{p,g}$	1000	J/(kg.K)
$C_{p,s}$	50	J/(kg.K)
d_p	0.001	M
ε_g (k < 150)	0.5	-
ε_g (k ≥ 150)	1.0	-
T_{inlet}	300	K
$T_{init.}$	100	K
Δz	0.002	m
u_z	6.0	m/s
Δt	0.0001	S
$\alpha_{gs}=6\varepsilon_s.Nu.k_g/(d_p)^2$	1664264.99	W/(m^3.K)

Table 2: Analytical solution for fixed bed test case.

$\xi=\frac{\alpha_{gs}}{\varepsilon_g\rho_g u_g C_{p,g}}z;\mathrm{t}'=\frac{\alpha_{gs}}{\varepsilon_s\rho_s C_{p,s}}(t-\frac{z}{u_g})$
$G(\xi,\mathrm{t}')=\frac{T_g-T_{init.}}{T_{g,inlet}-T_{init.}};P(\xi,\mathrm{t}')=\frac{T_s-T_{init.}}{T_{g,inlet}-T_{init.}}$
$G(\xi,\mathrm{t}')=1-e^{-\mathrm{t}'}\int_0^{\xi_z}I_0(\sqrt{4\mathrm{t}'\xi})e^{-u}d\xi$
$P(\xi,\mathrm{t}')=1-e^{-\mathrm{t}'}[\int_0^{\xi_z}I_0(\sqrt{4\mathrm{t}'\xi})e^{-u}d\xi+I_0(\sqrt{4\mathrm{t}'\xi_z})e^{-\xi_z}]$

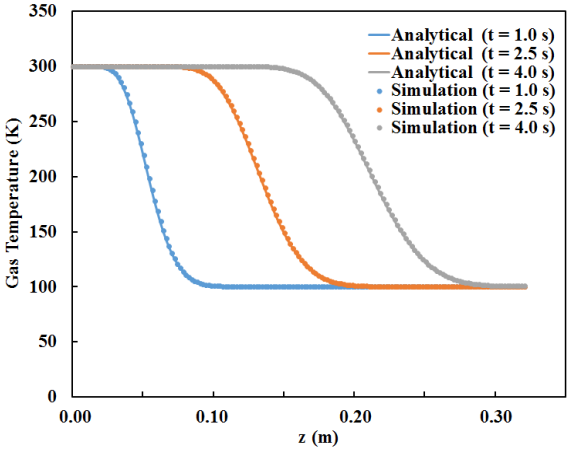

Figure 2: Comparison of the simulation results and the analytical solution for the case of plug flow in a fixed bed. The convection term has been discretised with Superbee scheme (Roe, 1986).

RESULTS

After successful implementation and verification of the energy equations into the existing code, detailed studies can be done. In this work, we study the bubble-to-emulsion heat transfer. To this end, we study several cases of the injection of a single hot (cold) bubble into a cold (hot) bed. The different simulation settings are summarized at Tables 3 and 4. It should be added that in all of these simulations, the amount of injected gas through nozzle is kept constant while changing the gas injected temperature. It is also assumed that the gas phase obeys the ideal gas law. Thus, if the injected gas temperature in case X is two times larger than the injected gas temperature in case Y, then the gas injection velocity in case X is also two times larger than its corresponding value in case Y (If the injection mass flux is the same in both cases). The simulations were performed at four different mass flux injections.

For the interpretation of the simulation results, we consider the energy balance over the injected bubble, which we may write as:

$$C_{p,b} m_b \frac{d(T_b)}{dt} = h_{BE} A_b (T_e - T_b) \tag{10}$$

After integration over time, following equations will be obtained.

$$h_{BE} = \frac{-C_{p,b} m_b}{A_b (t - t_{inj.})} \ln\left(\frac{(T_b - T_e)_t}{(T_b - T_e)_{t_{inj.}}} \right) \tag{11}$$

In this integration process, it is assumed that the bubble area does not change with time. As in the TFM simulations the bubble mass and area actually do change with time, their average values were used. It has to be added that the maximum absolute relative deviation of bubble mass to its average value in all the performed simulations were between 24.40-33.04% for 1.5 mm particles and 10.28-34.80% for 2.5 mm particles during the 0.04 seconds of integration. The corresponding deviations for bubble area is 14.36-29.30% and 14.18-37.82% for 1.5 mm and 2.5 mm particles respectively. Equation (11) is used to obtain the bubble-to-emulsion heat transfer coefficient by fitting the change of the normalized bubble temperature with time. The final results of h_{BE} for 1.5 mm and 2.5 mm particles at various injection velocities and injection temperatures are presented in Figure 3.

As it can be seen from Figure 3, h_{BE} increases linearly with bubble diameter which is in qualitative agreement with the model that is presented by Hartman et al. (2001), who also observed a linear increase of h_{BE} with increasing bubble diameter, up to d_B = 0.08 m. They observed a decrease in h_{BE} with bubble diameter for d_B>0.08. In our work, we do not observe a maximum in the bubble-to-emulsion heat transfer coefficient. This is probably due to the fact that in our work the bubble size was smaller than 0.08 m. On the other hand, this linear dependency is in disagreement with Kunii and Levenspiel model (1991) (KL model, refer to equation 12), where h_{BE} has a weak dependency to bubble diameter. It was also observed that the bubble-to-emulsion heat transfer coefficient increases with particle diameter. This observation can be explained by the fact that the bubble-to-emulsion mass exchange increases with particle diameter. This observation is in complete qualitative agreement with the Davidson-Harrison theory (Davidson and Harrison, 1993).

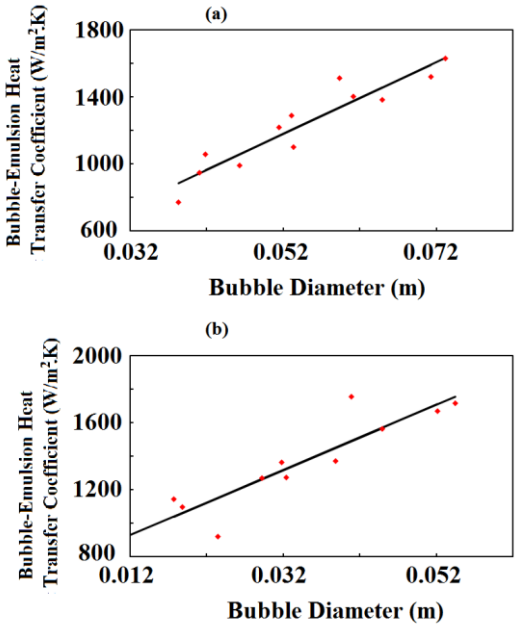

Figure 3: Bubble-emulsion heat transfer coefficient versus bubble diameter and the corresponding fitted line for **a.** d_p = 1.5 mm, $C_{p,g}$ = 1010 J/kg.K **b.** d_p = 2.5 mm, $C_{p,g}$ = 1010 J/kg.K.

The results of the TFM were also compared with the results of theoretical models in a quantitative way. The closest results to TFM results were obtained by KL model (1991). A comparison between the results of TFM and the KL model is presented in Figure 4. It should be added that the models that were proposed by Toei et al. (1972), Hartman et al. (2001) and Wu & Agarwal (2004) were the three other models which were investigated in this study. All these models gave results with no physical meaning. These disagreements can be due to a different range of applicability of their models with our simulations' conditions.

We note that the bubble velocity and bubble area required for the calculation of h_{BE} in the KL model were taken from the TFM results. As it can be seen from Figure 4, the TFM results and the results of the KL model have the same order of magnitude. It can also be seen that the differences increase with increasing bubble diameter. In all the cases, the KL model under-estimates h_{BE} for large bubbles and slightly over-estimates h_{BE} for small bubbles which may have large consequences in macroscopic models where a closure for h_{BE} is required. For this reason, a modification of the KL model is proposed in the next section.

MODIFIED MODEL FOR PREDICTION OF BUBBLE-EMULSION HEAT TRANSFER COEFFICIENT

Kunii and Levenspiel (1991) presented their model by the following equation:

$$H_{bc} = \frac{\upsilon C_{p,g} + h_{bc} S_{bc}}{V_b} \tag{12}$$

$$= 4.5 \frac{u_{mf} \rho_g C_{p,g}}{d_b} + 5.85 \frac{\left(k_g \rho_g C_{p,g}\right)^{1/2} g^{1/4}}{d_b^{5/4}}$$

where H_{bc} is the volumetric heat transfer coefficient, υ is the mass flow rate of gas from bubble to cloud, bc subscript indicates the bubble-cloud, V_b is the bubble volume and S_{bc} is the interfacial surface between bubble and cloud phases.

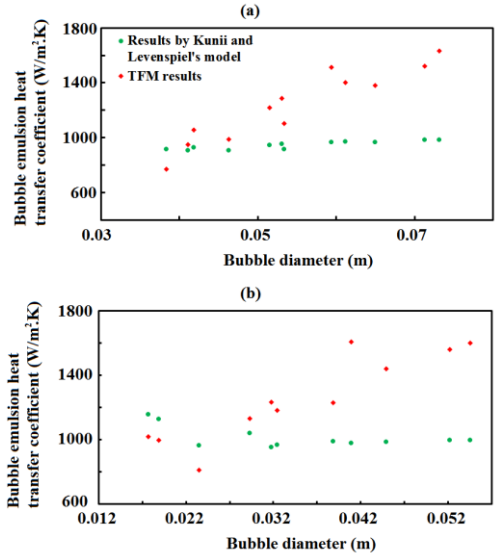

Figure 4: Comparison between the results of TFM and the KL model for **a.** d_p = 1.5 mm, $C_{p,g}$ = 1010 J/kg.K **b.** d_p = 2.5 mm, $C_{p,g}$ = 1010 J/kg.K.

The first term in the RHS of equation (12) is around two orders of magnitude larger than the second term in this equation. In other words, approximately

$$H_{bc} = 4.5\left(\frac{u_{mf}\rho_g C_{p,g}}{d_b}\right) \quad (13)$$

If it is assumed that bubbles have a spherical shape, bubble-emulsion heat transfer coefficient can be obtained by multiplying H_{bc} to the ratio of volume to surface of a sphere. In a mathematical word, $h_{BE} = 4.5\frac{u_{mf}\rho_g C_{p,g}}{6}$.

On the other hand, it is found out that bubble-emulsion heat transfer coefficient has a linear relationship with bubble diameter according to TFM results. This leads us to the point that the term $P = \frac{h_{BE,TFM}}{u_{mf}\rho_g C_{p,g}}$ should have a linear relationship with the bubble diameter. Figure 5 presents the dependency between these two parameters and fitted lines for 1.5 and 2.5 mm particles. The slope of these fitted lines give the correction factor for KL model. After fitting a function with the form of $P = \frac{h_{BE,TFM}}{u_{mf}\rho_g C_{p,g}} = \chi.d_B$, values of $\frac{6}{4.5}\chi.d_B$ were multiplied to the first term in KL model to get the modified model for prediction of bubble-emulsion heat transfer coefficient (χ is in m^{-1}). The final results of this analysis can be summarized by the following equation:

$$h_{BE} = 19.09(u_{mf}\rho_g C_{p,g} d_b) + \frac{5.85}{6}\frac{\left(k_g\rho_g C_{p,g}\right)^{1/2} g^{1/4}}{d_b^{1/4}} \quad (14)$$

$$= (19.09k_g)\,\mathrm{Re}_{b,mf}\,\mathrm{Pr} + \frac{5.85}{6}\frac{\left(k_g\rho_g C_{p,g}\right)^{1/2} g^{1/4}}{d_b^{1/4}}$$

The results of the modified model and its comparison with TFM results is presented in Figure 6. It should be noted that equation (14) is only valid for systems with d_p = 1.5-2.5 mm, ρ_p= 2526 kg/m^3, Pr = 0.86, d_B = 0.038-0.073 m (for 1.5 mm particles), d_B = 0.011-0.055 m (for 2.5 mm particles), $\mathrm{Re}_{b,mf}$ = 2302-4397 (for 1.5 mm particles) and $\mathrm{Re}_{b,mf}$ = 956-4879 (for 2.5 mm particles). Using of this equation for other conditions needs further investigation especially for larger bubbles as the dependency of h_{BE} to d_B may change.

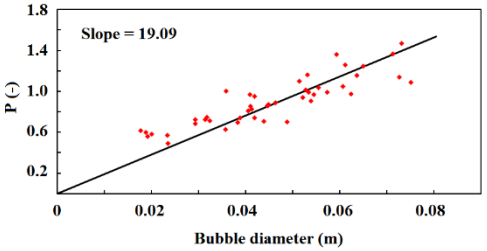

Figure 5: Dependency of $\frac{h_{BE,TFM}}{u_{mf}\rho_g C_{p,g}}$ to bubble diameter for 1.5 mm and 2.5 mm particles.

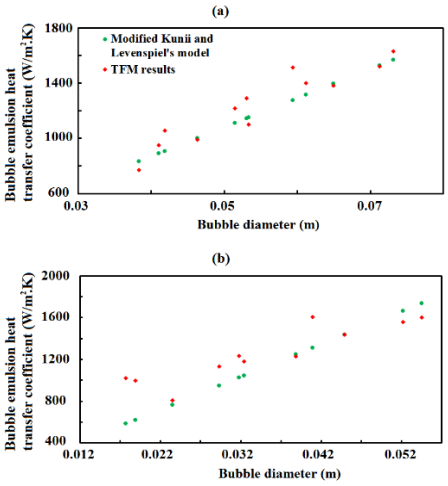

Figure 6: Comparison between h_{BE} from TFM and h_{BE} from modified KL model: **a.** d_p=1.5 mm, $C_{p,g}$ = 1010 J/kg.K, **b.** d_p = 2.5 mm, $C_{p,g}$ = 1010 J/kg.K

CONCLUSION

Implementation and verification of the thermal energy equations into an existent TFM code were done successfully. Subsequently, simulations were done for the injection of a single hot/cold bubble into a bubbling fluidized bed. The simulation data was used to numerically calculate the bubble-to-emulsion heat transfer coefficient. It is found that the bubble-emulsion heat transfer coefficient increases with bubble and particle diameter. This observation was in qualitative agreement with findings by Hartman et al. (2001) and Wu & Agarwal (2004). The results were also compared with theoretical models. None of the models except the model of Kunii and Levenspiel (1991) were suitable for predicting h_{BE} as they were developed for fine particles. Kunii and Levenspiel model could give reasonable results. However, the dependence of bubble-emulsion heat transfer coefficient on the bubble diameter was not predicted well by Kunii

and Levenspiel model. Therefore, in this work a modified model was proposed that can be used as an input for large-scale phenomenological models of fluidized beds with coarse particles.

Table 3: Schematic representation and boundary conditions for simulations.

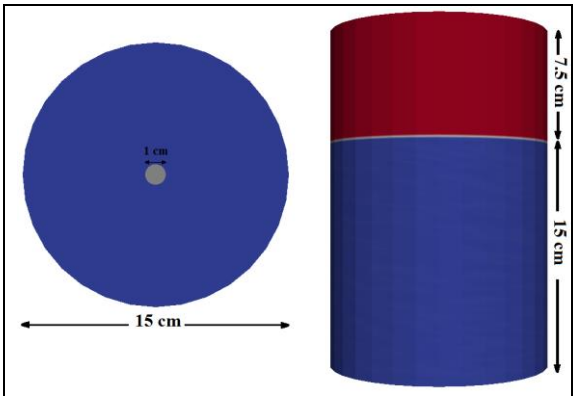

Boundary Conditions:

- Wall of the cylinder: no slip for gas and partial slip for particles
- Axis of the cylinder: free slip for both phases
- Outlet: prescribed atmospheric pressure
- Inlet: prescribed gas influx

Table 4: Simulations' conditions for isolated hot (cold) rising bubble.

Variable	Value	Unit
$C_{p,g}$	1010	J/(kg.K)
$C_{p,s}$	840	J/(kg.K)
d_p	0.0015, 0.0025	m
u_{inj}	10, 15, 20, 30	m/s
u_{bg}	0.94, 1.40	m/s
μ_g	1.83×10^{-5}	Pa.s
t_{inj}	0.1	s
MW_g	28.8	kg/kmol
k_s	1.04	W/(m.K)
k_g	0.0214	W/(m.K)
ρ_s	2526	kg/m^3
e	0.97	s
Δt	4×10^{-6}	s

ACKNOWLEDGEMENTS

This work is part of the Research Programme of Dutch Polymer Institute (DPI) as a project number # 751.

REFERENCES

BIYIKLI, S., TUZLA, K., CHEN, J.C., (1989), "A phenomenological model for heat transfer in freeboard of fluidized beds". *Can. J. Chem. Eng.*, **67**, 230-236.

DAVIDSON, J.F. and HARRISON, D., (1993), "Fluidised Particles". *Cambridge University Press*.

GENG, Y. and CHE, D., (2011), "An extended DEM-CFD model for char combustion in a bubbling fluidized bed combustor of inert sand". *Chem. Eng. Sci.*, **66**, 207–219.

GIDASPOW, D., (2012), "Multiphase Flow and Fluidization: Continuum and Kinetic Theory Descriptions".

GUNN, D.J., (1978), "Transfer of heat or mass to particles in fixed and fluidized beds". *Int. J. Heat Mass Transfer*, **21**, 467-476.

HARTMAN, G., WU, W.Y., CHEN, Z.M. and AGARWAL, P.K., (2001), "Heat transfer between an isolated bubble and the dense phase in a fluidized bed". *Can. J. Chem. Eng.*, **79**, 458–462.

KANEKO, Y., SHIOJIMA, T. and HORIO, M., (1999), "DEM simulation of fluidized beds for gas-phase olefin polymerization". *Chem. Eng. Sci.*, **54**, 5809–5821.

KUIPERS, J.A.M., VAN DUIN, K.J., VAN BECKUM, F.P.H. and VAN SWAAIJ, W.P.M., (1993), "Computer simulation of the hydrodynamics of a two-dimensional gas-fluidized bed". *Comput. Chem. Eng.*, **17**, 839–858.

KUNII, D., LEVENSPIEL, O., (1991), "Fluidization Engineering".

NIEUWLAND, J.J., VEENENDAAL, M.L., KUIPERS, J.A.M. and VAN SWAAIJ, W.P.M., (1996), "Bubble formation at a single orifice in gas-fluidised beds". *Chem. Eng. Sci.*, **51**, 4087–4102.

ROE, P., (1986), "Characteristic-based schemes for the Euler equations". *Annu. Rev. Fluid Mech.*, **18**, 337–365.

SRIVASTAVA, A. and SUNDARESAN, S., (2003), "Analysis of a frictional-kinetic model for gas-particle flow". *Powder Technol.*, **129**, 72–85.

TOEI, R., MATSUNO, R., HOTTA, H., OICHI, M. and FUJINE, Y., (1972), "The capacitance effect on the transfer of gas or heat between a bubble and the continuous phase in a gas-solid fluidized bed". *J. Chem. Eng. Japan*, **5**, 273–279.

VAN DER HOEF, M.A., YE, M., VAN SINT ANNALAND, M., ANDREWS, A.T., SUNDARESAN, S. and KUIPERS, J.A.M., (2006), "Multiscale modeling of gas-fluidized beds". *Adv. Chem. Eng.*, **31**, 65–149.

VERMA, V., DEEN, N.G., PADDING, J.T., KUIPERS, J.A.M., (2013), "Two-fluid modeling of three-dimensional cylindrical gas-solid fluidized beds using the kinetic theory of granular flow". *Chem. Eng. Sci.*, **102**, 227-245.

WU, W. and AGARWAL, P.K., (2004), "Heat transfer to an isolated bubble rising in a high-temperature incipiently fluidized bed", *Can. J. Chem. Eng.*, **82**, 399–405.

ZEHNER, P., Schlunder, E.U., (1970), "Warmeleitfahigkeit von schuttungen bei massigen temperaturen". *Chemie Ing. Tech.*, **42**, 933-941.

